

Definition of the Oxygen A-Band Channels of ENVISAT's 'Medium Resolution Imaging Spectrometer' for Cloud Monitoring

by

M. KOLLEWE[†], J. FISCHER[‡]

[†]Universität Hamburg, Meteorologisches Institut¹

[‡]Freie Universität Berlin, Institut für Weltraumwissenschaften, Germany

Abstract

During the 'European Lidar Airborne Campaign' (ELAC) in 1990 the backscattered sunlight in the region of the O₂ A-band at $0.76\mu m$ was measured above various clouds. The multispectral radiance measurements were performed with a nadir-looking device with a spectral resolution of $\Delta\lambda = 0.42nm$. A 'Principal Component Analysis' (PCA) was applied to about 140000 spectra, each consisting of 320 channels. It turns out that above clouds with optical depths $\delta_C > 10$ or above clouds over oceans *three* spectral regions with $\Delta\lambda \approx 2.5 - 5nm$ contain the entire information of the high-resolved spectra. One of these intervals is located near the absorption band (window channel) while the remaining two cover the *R*- and the *P*-branch of the O₂ A-band, respectively. Based on this finding, the O₂ A-band channels of the planned 'Medium Resolution Imaging Spectrometer' (MERIS, ESA), dedicated to the detection of the cloud-top height, are defined.

1 Introduction

There is no doubt about the importance of clouds for weather formation and climate effects^{[9],[11]–[14]}. However, an instrument for detection of the cloud-top height z_{top} with the desired accuracy is still

¹Now at: Universität Hamburg, II. Institut für Experimentalphysik. Mail-adress: Universität Hamburg, Fachbereich Informatik (KOGS), Vogt-Kölln-Straße 16, 22527 Hamburg, Germany

to be expected. In 1998 ESA's 'Environmental Satellite' (ENVISAT) is planned to be launched with the 'Medium Resolution Imaging Spectrometer' (MERIS) on a polar orbit. Besides MERIS contribution to ocean-colour measurements, it will also provide data on clouds and aerosols. For the measurement of z_{top} it is planned to use the gas-absorption of oxygen within its A-band near $0.76\mu m$. This principle was first proposed by Yamamoto and Wark (1961) who answered to a suggestion of Hanel (1961) to use the CO_2 band at $2-2.1\mu m$ for that purpose. The idea is to measure the absorption of the sunlight backscattered from clouds into space within an absorption band. The amount of absorption depends on the thickness of the atmospheric layer above the cloud. Thus, z_{top} can be calculated if the absorption is estimated. However, not only absorption above the cloud appears but also *within* and *beneath* the cloud^{[5][6]}. It turns out, that more information is needed, thus more than one channel has to be placed within the O_2 A-band to face this problem.

Figure 1 shows the oxygen A-band measured by Delbouille et al. (1981). The new generation of imaging spectrometers like MERIS provide spectral resolutions, which allow to resolve this band to some extent. The open questions are how many independent pieces of information on cloud-top retrieval are achievable and *where* to place *how many* channels with *which spectral width* in the region of the O_2 A-band to optimize this MERIS-application.

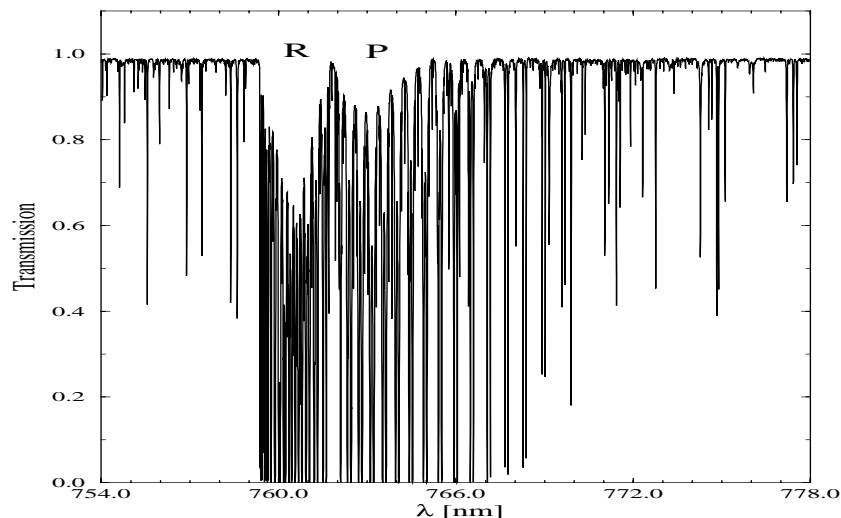


Figure 1: Atmospheric transmission at the Jungfrauoch (Delbouille et al., 1981). Spectral resolution $\Delta\lambda = 10m\text{\AA}$.

2 Measurements

During the 'European Lidar Airborne Campaign 1990' (ELAC 1990) a grating spectrometer, an *Optical Multichannel Analyser* (OMA), was used to measure the spectral signature of the upwelling sunlight reflected by the cloud-top. The O_2 A-Band was measured with a spectral resolution of

$\Delta\lambda = 0.42nm$ in 320 channels (channel-distance $\approx 0.1nm$) and exposure times varied between 100 and 300ms. The OMA was mounted nadir-looking onboard the FALCON 20 jet of the *Deutsche Forschungsanstalt für Luft- und Raumfahrt* (DLR). Seven flights were performed between the 09. to the 25. October 1990. Their locations and flight-numbers are illustrated in Figure 2.

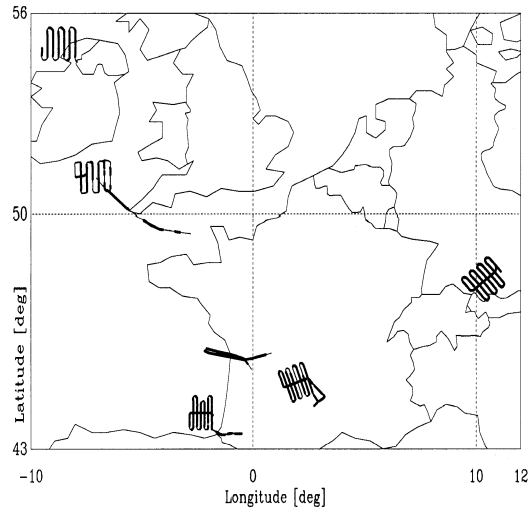


Figure 2: Patterns and location of seven ELAC 1990 missions where OMA was operated.

During the flights, cloudless tracks were passed as well as different cloud types (Pure Stratus, Altostratus, Cumulus, Stratocumulus, Altocumulus, Cirrus and multilayered situations). Approximately 140000 spectra over clouds could be registered.

3 Analysis and Results

The first step of the analysis of the O_2 A-band spectra taken during ELAC 1990 was to normalize all spectra with respect to the window radiances just outside the band to eliminate effects which are not due to O_2 absorption. A 'Principal Component Analysis' (PCA) was then applied to the normalized spectra. In that manner *two* principal components (= independent effects on the spectral signature) could be found (Figure 3). While the first one has the same sign for the two branches of the band, the second has the opposite sign for the *P*- and *R*-branch.

The interpretation of these effects lead to three atmospheric parameters involved. The first principal component (Figure 3a) expresses the changing mean absorption due to changing absorbermasses (i.e. changing z_{top} and cloud thicknesses). The second principal component (Figure 3b) is probably due to the influence of pressure and temperature on the absorption: Figure 4 reproduces two *simulations* of the O_2 A-band OMA-measurements (= averaged with a gauss-function with half-width $0.42nm$ such as the OMA spectral response function) with the same $z_{top} = 8.12km$ and the

same optical thickness $\delta_C = 13.75$. When the geometrical thickness is changed from $\Delta z = 5.62km$ to $\Delta z = 1.36km$ while the surface albedo is increased from ocean to land the absorption over the entire band remains approximately the same (= *no* change of the *first* principal component) but there is an effect on the the *second* principal component. The weighting function changes from upper atmospheric levels in the first case to lower levels with higher pressures and temperatures in the second case which means that the effects of pressure and temperature differ in both cases, while the mean absorption is approximately the same.

The effect described above offers the possibility to get some information about the vertical distribution of the optically relevant cloud parameters and thus to get a measure of the extinction coefficient or penetration depth of the light.

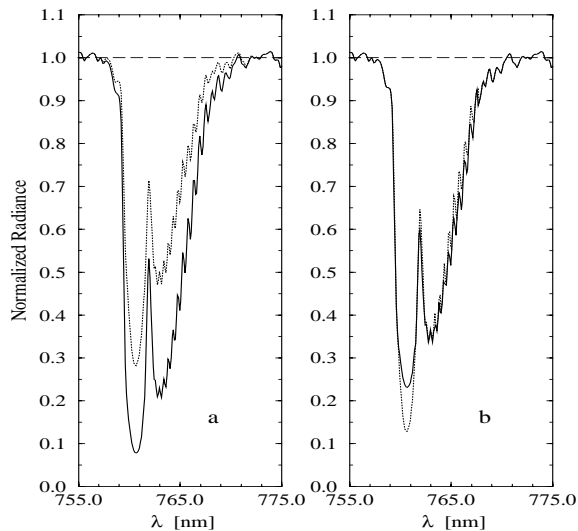


Figure 3: Two independent effects on spectral signature of the O₂ A-band found by PCA of the ELAC 1990 spectra.

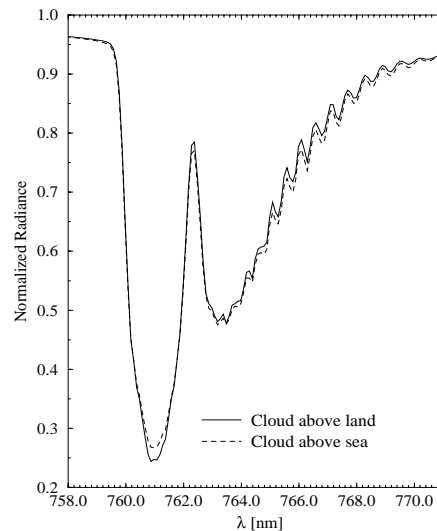


Figure 4: Simulated normalized radiance above a cloud of $z_{top} = 8115m$ and $\delta_C = 13.75$
 - - - : surface ocean, wind speed $7m/s$, $\Delta z = 5616m$ ($\beta_C = 2.45/km$) — : surface land, spectral albedo $a=0.2$, $\Delta z = 1359m$ ($\beta_C = 10.12/km$)

4 Application to MERIS channels and Discussion

Based on the results of PCA the possible MERIS-channels for using O₂ A-absorption as a means of detection of z_{top} could be defined. Detailed investigations have shown, that at least over optically thick clouds or over ocean *one* reference channel outside the band is sufficient (Kollewe and Fischer, 1994a). Furthermore, PCA has shown that *two* independent effects are found within the *normalized* spectra, i.e. *two* channels have to be placed within the O₂ A-band, see Figure 3. For this investigation

possible MERIS channels were simulated by using the high resolved OMA spectra and averaging over wavelength while the information content remains.

When the possible channels of MERIS within the O₂ A-band were defined by averaging over wavelength, some limitations had to be accounted for:

- The number of channels is restricted.
- The channels can be created by grouping the array diodes of the chip. A group (\equiv channel) has to consist of at least two diodes.
- The locations of the photo diodes on the λ -scale and their widths are given. The edges λ_i of the diodes in vacuum lie at wavelengths described by

$$\lambda = 400.0nm + i 1.25nm \quad (1)$$

Figure 5 shows the three (two within the band plus one reference window channel) channels, related to the eigenvectors found by PCA (upper curves).

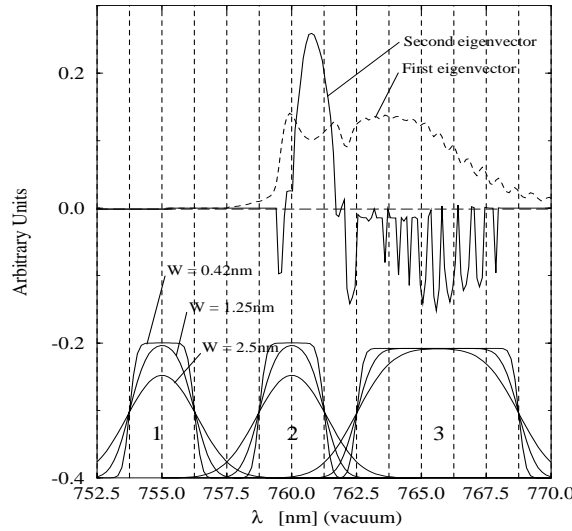


Figure 5: Proposed channels with different spectral resolutions of MERIS, vertical lines indicate the edges of the photodiodes on the diode-array in vacuum.

The vertical dashed lines illustrate the locations and widths of the photodiodes of the MERIS chip. The channels are created by grouping several photodiodes ($=$ rectangular function) and the convolution with the filter function of the spectrograph optics which is assumed to be gaussian. The results of three different half-widths of the gaussian function are shown in the lower part of Figure 5.

As a test a further PCA was performed with the averaged 'MERIS' spectra, gained by averaging the OMA spectra as shown in Figure 5. In opposite to the first PCA no normalization was done at

first and only spectra over ocean were taken into account. In Table 1 the square-roots of resulting eigenvalues are listed for the three different resolutions shown in Figure 5. The corresponding eigenvectors are reproduced in Figure 6.

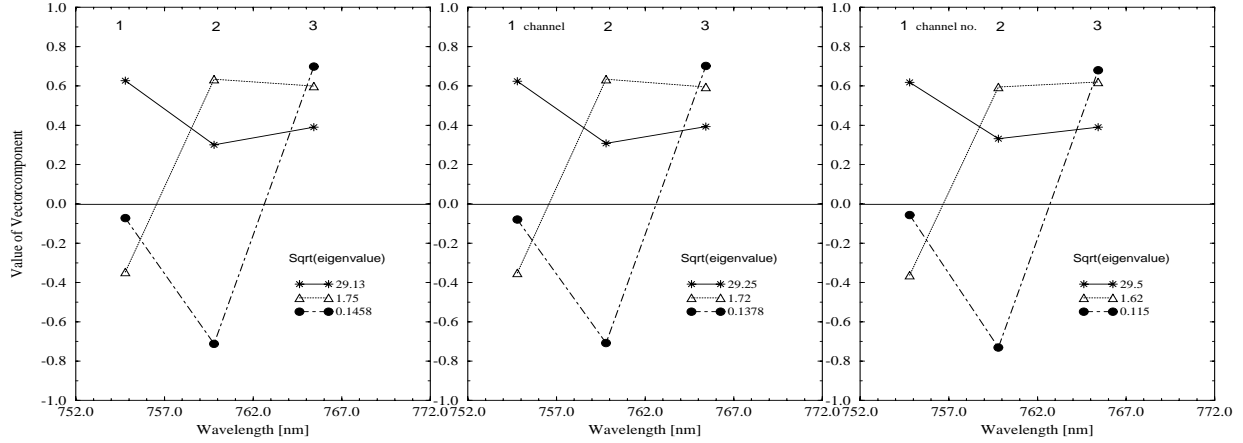


Figure 6: Resulting eigenvectors, when PCA is applied to ELAC 1990 spectra which are averaged with different filter-functions according to Figure 5

Now the first eigenvalue and -vector (same sign for all channels) is caused by the total spectral albedo, which was eliminated by normalization before. The remaining eigenvalues and -vectors are already known from the analysis of the high resolved spectra: while one has same sign for the two O_2 A-band branches, the other (now the third) shows the characteristic change of sign.

Table 1: Square-roots of eigenvalues of spectra averaged after Figure 5

	$W_{Gauss} = 0.42nm$	$W_{Gauss} = 1.25nm$	$W_{Gauss} = 2.5nm$
$\sqrt{Eigenvalue1}$	29.13	29.25	29.5
$\sqrt{Eigenvalue2}$	1.75	1.72	1.62
$\sqrt{Eigenvalue3}$	0.1458	0.1378	0.115

Table 1 shows, that obviously the width of the gauss-function (the spectral resolution) plays a minor role compared to the location of the channels. A drastic change of W_{Gauss} from $0.42nm$ (OMA-resolution) to $2.5nm$ causes a change in $\sqrt{Eigenvalue3}$ of about 20%.

Based on the findings presented here, a cloud-top height algorithm was defined which follows the principle of *inverse modeling*. This algorithm uses the measured radiance in 'MERIS' channels 1-3, gained by averaging the OMA measurements, and computes the three cloud parameters δ_C , z_{top} and Δz . By comparison of the 'MERIS'-results of z_{top} with Lidar measurements of z_{top} , which also had been taken during ELAC 1990, it could be shown, that the remote sensing of δ_C , z_{top} and Δz can be realized by using L_1 , L_2 and L_3 (Kollewe and Fischer, 1994b).

However, when comparing the simulations with measurements, a discrepancy appeared, which could not yet be explained (Figure 7).

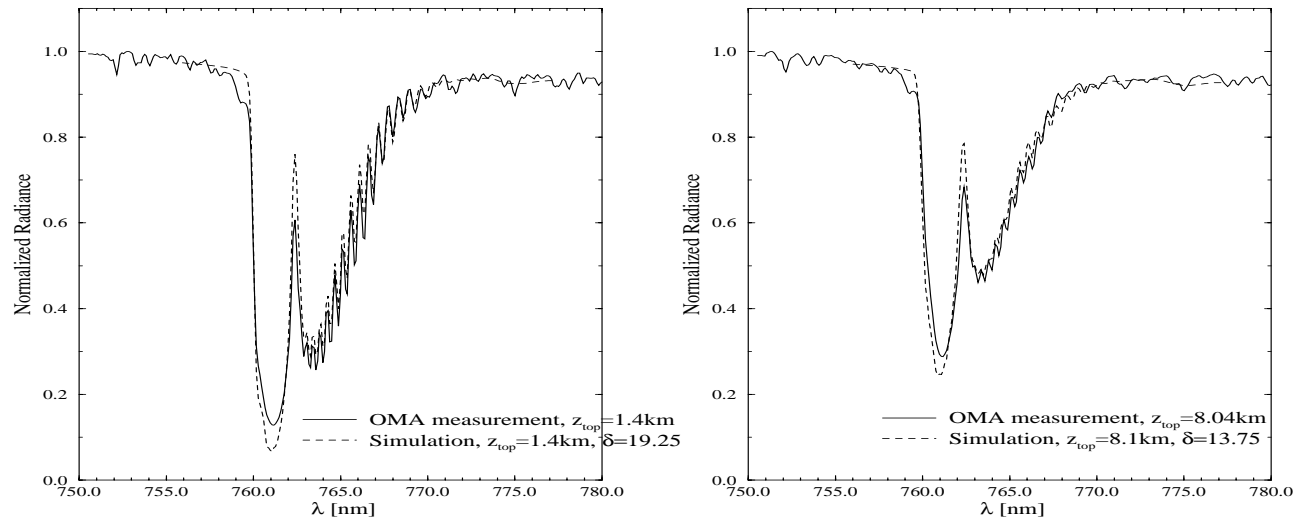


Figure 7: Discrepancy between simulations and measurements with respect to differences in absorption within the two branches of the oxygen A-band. a) Flight 1730, 09. October 1990, 10:23:00h UT, Stratus over sea. b) Flight 1738, 19. October 1990, 09:55:30h UT, Altocumulus over sea.

When comparing the simulated and measured normalized high resolved spectra of the O_2 A-band for a given situation and adjusting the model cloud Δz in that way, that the total absorption agrees, in every case, the signal in the R -branch is too low while the signal in the P -branch is too high for the simulations. Neither tests with a 10% change of the half-widths of the O_2 absorption lines nor tests with drastic changes of the temperature profiles of the model-atmospheres could explain the differences. A possible explanation is, as proposed by Adiks and Dianov-Klokov (1968) and Adiks et al. (1972) not to use the common Lorentz shape to represent the shape of the single O_2 lines but a slightly different one. Thus, if the line wings are emphasized, the signal in the P -branch is lowered relative to the signal in the R -branch due to the smaller compactness of the lines in the P -branch.

Systematic differences between O_2 A-band measurements and simulations were also found by Pflug (1993). He also assumes uncertainties in the knowledge of the line parameters or line shapes as the error source.

5 Acknowledgements

We wish to thank the GKSS-Forschungszentrum and the Deutsche Forschungsanstalt für Luft- und Raumfahrt for the cooperation during the measurement campaign. This work has been supported by the Deutsche Forschungsgemeinschaft and the European Space Agency.

References

- [1] Adiks, T.G., V.I. Dianov-Klokov (1968): Molecular parameters of the O₂ absorption band at 0.762 μ m and their use in calculating the transmission function; *Atm. Ocean Phy.*, **4**, 10, 605-609.
- [2] Adiks, T.G., Y.S. Georgiyevskiy, M.S. Malkevich, N.S. Filippova (1972): Atmospheric transmission in the 0.76 μ m O₂ band; *Atm. Ocean Phy.*, **8**, 4, 210-216.
- [3] Hanel R. A. (1961): Determination of Cloud Altitude from a Satellite; *J. Geophys. Res.*, **66**, 4, 1300.
- [4] Delbouille L., G. Roland, L. Neven (1981): Photometric atlas of the solar spectrum from $\lambda = 3000$ to $\lambda = 10000\text{\AA}$; Liege: Institut d'Astrophysique de l'Université, Observatoire Royal de Belgique, [Data-Tape].
- [5] Fischer J., H. Graßl (1991): Detection of Cloud-Top Height from Backscattered Radiances within the Oxygen A Band. Part 1: Theoretical Study; *J. Appl. Meteor.*, **30**, 9, 1245–1259.
- [6] Fischer J., W. Cordes, A. Schmitz-Peiffer, W. Renger, P. Mörl (1991): Detection of Cloud-Top Height from Backscattered Radiances within the Oxygen A Band. Part 2: Measurements; *J. Appl. Meteor.*, **30**, 9, 1260–1267.
- [7] Kollewe, M., J. Fischer (1994a): Use of the Oxygen A Band for Cloud-Top Height Determination: Measurements and Simulations; Submitted to: *J. Appl. Meteor.*
- [8] Kollewe, M., J. Fischer (1994b): Use of the Oxygen A Band for Cloud-Top Height Determination: Application to a Coarse Spatial Resolution Imaging Spectrometer; Submitted to: *J. Appl. Meteor.*
- [9] Ohring, G., S. Adler (1978): Some Experiments with a Zonally Averaged Climate Model; *J. Atmos. Sci.*, **35**, 186–205.
- [10] Pflug, B. (1993): Atmospheric transmission in the O₂ A-band: Comparison of calculations and measurements; Workshop Proceedings *Atmospheric Spectroscopy Applications - ASA Reims 93*, University of Reims, France, p. 68-71
- [11] Ramanathan V., D. Cess, E. F. Harrison, P. Minnis, B. R. Barkstrom, E. Ahmad, D. Hartmann (1989): Cloud-Radiative Forcing and Climate: Results from the Earth Radiation Budget Experiment; *Science*, **243**, 59–63.

- [12] Raval A., V. Ramanathan (1989): Observational Determination of the Greenhouse Effect; *Nature*, **342**, 758–761.
- [13] Roeckner E., U. Schlese, J. Biercamp, P. Löwe (1987): Cloud optical depth feedbacks and climate modeling; *Nature*, **329**, 138–140.
- [14] Stephens, G. L., T. J. Greenwald (1991): The Earth’s Radiation Budget and Its Relation to Atmospheric Hydrology. 2. Observations of Cloud Effects; *J. Geophys. Res.*, **96**, D8, 15325–15340.
- [15] Yamamoto G., D. Q. Wark (1961): Discussion of the Letter by R. A. Hanel, ‘Determination of Cloud Altitude from a Satellite’; *J Geophys Res*, **66**, 10, 3596.